Dynamic scaling of island-size distribution in submonolayer growth of 1×1 films

Q. Jiang, A. Chan, and G.-C. Wang
Physics Department, Rensselaer Polytechnic Institute, Troy, New York 12180-3590
(Received 9 June 1994)

The scaling of island-size distribution of an epitaxially grown 1×1 Fe film on a Au (001) surface as a function of coverage was observed using high-resolution low-energy electron diffraction. The scaling function extracted from the intensity distribution of integer-diffracted beams is best described by a γ function. The island density is almost a constant in the aggregation growth regime. The forms of the scaling function and the island density are in qualitative agreement with recent simulations of molecular-beam-epitaxy growth.

I. INTRODUCTION

The dynamics of submonolayer ordering has attracted great interest recently.[1,2] Submonolayer growth processes include nucleation, growth, and coalescence of islands with diverse symmetries and degeneracies. In nonequilibrium submonolayer growth, one may study the island size and density as a function of time t or coverage θ, and temperature T. For a fixed coverage, one may quench a system from a disordered state at an initial temperature, which is far from equilibrium, to a state at a final temperature where a pattern consisting of islands develops as a function of time. The pattern is characterized by a time-dependent length scale (island size) $R(t)$ and a size distribution $P[R(t)]$. The dynamical scaling hypothesis[1,2] implies that there is only one length scale, which grows as a power law in time $R(t)\sim t^n$ and that the distribution function remains invariant after rescaling, i.e., $P'(x)\sim[1/R'(t)]P[R(t)]$, where R' is the average island size and x is R/R'. The value of the exponent n reveals the growth mechanism.[3–6] For example, at saturation coverage of a particular superstructure, the growth mechanism may be curvature driven if $n=\frac{1}{2}$. In this paper, we present the first observation of dynamic scaling of 1×1 island-size distribution as a function of coverage θ. In this mode, we study the change of submonolayer pattern as we continuously add atoms to 1×1 islands at a fixed temperature. We observe that the island size grows as a function of coverage following a power law: $R(\theta)\sim\theta^n$ and the corresponding island-size distribution rescales as $P'(x)\sim[1/R'(\theta)]P[R(\theta)]$. The island density obtained is almost constant revealing an aggregation growth regime.

The study of submonolayer growth of films became practical with real-space imaging techniques such as scanning tunneling microscopy (STM). Valuable information such as island shape, island density and distribution, and spacing between islands can be imaged. The activation energy and the prefactor of diffusion constant can be analyzed from the images.[7,8] In this paper, we present a method that uses reciprocal space techniques (electron, x-ray, and He atom-beam diffraction) to measure the intensity distribution or angular profiles of integral-order beams scattered from a 1×1 film. The result provides not only the island-size distribution but also the spacing (between edges of adjacent islands) distribution of 1×1 films. The scaling of island-size distribution that we obtained using high-resolution low-energy electron diffraction (HRLEED) is equivalent to a statistical ensemble average of about 10^8 STM images. The study of 1×1 island is a particularly challenging problem because there are no superlattice diffraction beams formed after atoms are deposited on the surface, i.e., we study a 1×1 epitaxial layer, which gives a 1×1 LEED pattern. With a superlattice beam present, one can separate the contribution from islands and the contribution from spacings (unoccupied regions) because the superlattice beam intensity is due to interference from incoherent islands only.[9,10] The spacings between islands that are one level (one step) lower are not considered. Instead, for the 1×1 pattern, one has to measure the angular intensity profiles of integral-order beams, which contain interference from *both* islands and substrate space (with no occupation of adsorbed atoms). Experimentally one needs to measure the profile changes in integral-order diffraction beams. If the change in the intensity profile is not obvious, one may not gain any new information about the growth. In our case, the high resolution of the instrument (6×10^{-3} Å^{-1}) detects the change of profile as a function of coverage clearly. A direct comparison of the measured profiles indicates qualitative shape changes. This is fundamentally different from the cases where measured profile shapes from superlattice beams look qualitatively similar.[9,10] The scaling function we obtained is also consistent with recent molecular-beam-epitaxy model simulations.[1,2] To the best of our knowledge this is the first quantitative study of the scaling behavior of 1×1 islands as a function of submonolayer coverage.

II. EXPERIMENT

The submonolayer Fe films were prepared in an ultrahigh-vacuum chamber equipped with a high-resolution LEED, an Auger electron spectrometer (AES), a sputtering gun, and an electron-bombardment evaporation source made of Fe foil. The details of the Fe evaporation source, Au substrate characterization, and coverage determination have been presented before and will

not be repeated here.[11] The lattice constants of Fe and Au differ by 0.4% and a 1×1 pattern is always formed at all coverages we studied. All the data presented are for films grown at room temperature. No carbon or oxygen contamination was detected in the films within the sensitivity of our AES.

III. RESULTS AND DISCUSSIONS

Before the Fe depositions, the substrate Au(001) shows a 5×1 reconstruction pattern. The angular intensity distribution of the (00) beam along one azimuthal direction at $E=27.5$ eV, an out-of-phase condition, is shown in Fig. 1(a). The intensity distribution is the instrument response function convoluted with the physical signal from the finite terrace size of Au ($\sim$600 Å). Figures 1(b), 1(c), and 1(d) show the (00) beam profiles after 5, 8, and 11 sec of Fe depositions, respectively. The Au surface reconstruction disappears after these depositions. The profile changes from the Gaussian-like profile of the clean surface into a spike on shoulder structure. Further deposition decreased the central spike intensity and eventually a split profile was observed. Continuous depositions reversed the trend of profile change and a Gaussian-like profile was obtained again at the completion of 1 ML. This latter half of our data is not shown here. All the profiles shown here are one-dimensional cuts through two-dimensional symmetric profiles. Similar data were reproduced with different deposition rates.

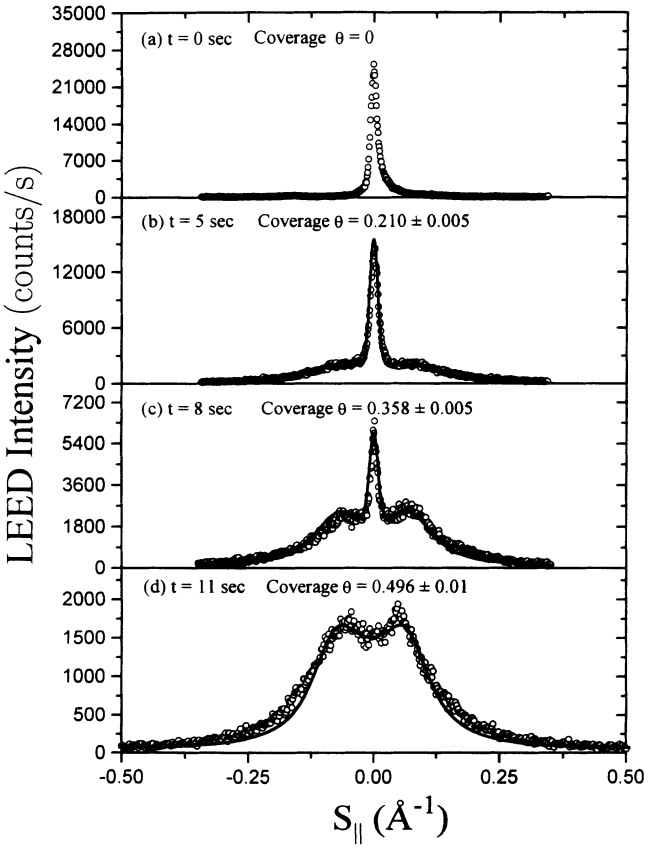

FIG. 1. The coverage-dependent angular intensity distribution of the (00) diffraction beam measured at the out-of-phase condition. The angle has been converted into $S_{\|}$, the momentum transfer parallel to the surface. The solid curves are the calculated angular profiles using coverages, island size, and spacing distributions as parameters.

A. Determination of a two-level system

One important question in the study of the initial stage of growth is whether the growth is layer-by-layer or two level in the first layer, or instead multilevel three-dimensional (3D) islanding. Many adsorbates form 3D islands especially when the adsorbates have high surface free energy compared with that of the substrate or when the Schowebel barrier is high.[12] In practice, one can determine a surface morphology with arbitrary island size or spacing distributions in a finite number of levels from diffraction profiles, which are Fourier transforms of the pair-correlation function. The analysis of integer-order diffraction beams from a 1×1 pattern is not trivial. One requires a high-resolution diffractometer to detect minute changes in the integer-order beam profiles if only a 1×1 pattern is involved. Pimbley and Lu[13] developed a scheme that allows the calculation of exact and analytic atomic-pair correlation function (one-dimensional) from an arbitrary distribution of island sizes and an arbitrary distribution of substrate terrace widths (the unoccupied regions) in a finite number of epitaxial layers. The inclusion of unoccupied regions introduces the interference between islands and substrates and gives destructive as well as constructive scatterings when electron wavelength varies. Therefore, the time-dependent (see Fig. 1) and energy-dependent (see Fig. 2) profiles show a series of qualitative changes. We apply this scheme to the 1×1 overlayer structure in a two-level submonolayer regime.

We have used two ways to confirm that the submonolayer we prepared is a two-level system. One way is the G-factor analysis[14] in which the vertical layer distribution can be obtained as shown in the inset of Fig. 3. The details of island size and spacing distributions are not needed in the G-factor analysis. In this analysis, one assumes that the LEED intensity can be split into the dynamic-form factor F and lattice G factor. The lattice factor depends only on the equilibrium surface atom positions for atoms arranged in a periodic lattice horizontally and vertically in the surface. An integration of the lattice G factor over the Brillouin zone (BZ) equals one. The G factor is obtained by dividing the peak intensity of a profile by the integrated intensity over the BZ. If the form factor does not change over the BZ, then an average form factor can be separated from the G factor and pulled out from the integral. Therefore, the form factor at the peak cancels the average form factor in the denominator and leaves us with a G factor. We have analyzed the energy-dependent profiles this way and calculated the G factor theoretically using the coverages at different levels as parameters. The result obtained for 11 sec deposition is shown in Fig. 3. This plot shows that the G factor has its minimum at 3π and 5π, the out-of-phase condition, and its maximum at 4π, the in-phase condition. The upper-corner inset shows the vertical-layer distribution

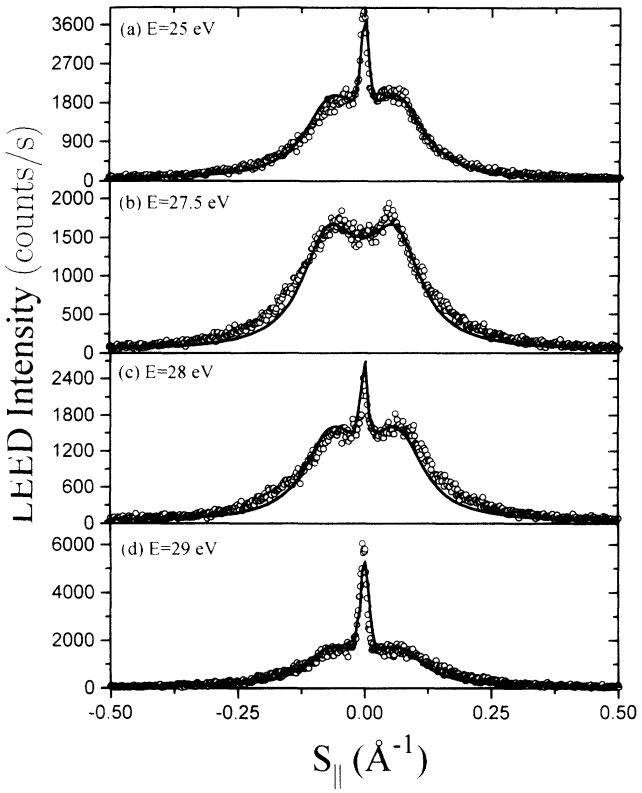

FIG. 2. The energy-dependent angular intensity distribution of the (001) diffraction beam measured at about 0.5 ML coverage. The solid curves are calculated angular profiles using the same parameters as in Fig. 1(d).

used in the calculation: the first layer coverage, 0.50±0.01 ML, and all other levels, zero coverages. Any other combination of layer distribution gives a poorer fit. This result confirms that the deposited film is a two-level system. Another way is to plot the distance between the two shoulders of the profiles measured at various energies shown in Fig. 4. The almost constant separation in reciprocal space over a wide range of energy (phase) implies a two-level system.[13]

B. Island-size distribution and scaling

To study the details of island size and spacing distributions in the submonolayer regime, we need to calculate the diffraction profiles and compare with the measured profiles. The essence of the theoretical simulation of a 1×1 diffraction profile from a two-level system is described below. One first writes down the diffracted intensity at a fixed energy,[13] which contains parameters such as coverage θ, Fourier transform of island-size distribution $P_a(R)$, and spacing distribution $P_s(R)$. (The subscripts a and s denote island and spacing, respectively.) Then one assumes distributions $P_a(R)$ and $P_s(R)$, which could be any function in units of lattice constant a ($=2.88$ Å). Next, integrate the transform of the distributions and substitute it back to the diffraction intensity. Finally, calculate the angular profiles and compare them with the measured angular profiles. Various distributions have been tried in the calculation of diffraction intensity. The calculations using Γ distributions $[P(R)=Z\sum_{N=1}^{\infty}R^{j}e^{-\omega R}\delta(R-Na)$, where Z is a normalization constant and N is an integer] for both island sizes and spacings give the best fits, which are shown as solid curves in Fig. 1. There are two parameters in the Γ distribution, j and ω. The use of Γ distribution and the choice of parameters, j and ω has been optimized not only by the fit of profiles shown in Fig. 1 but also the profiles obtained for a series of energies away from 27.5 eV (over 60 profile fits, some presented in Fig. 2). The j_a is 2 and the ω_a are 0.078, 0.060, and 0.050 for 5, 8, and 11 sec, respectively. (The subscript a is for adatoms.) Judging from Fig. 1, one can see that the fits reproduce the qualitative change in the measured profiles. From these fits, the coverages are also obtained. When the split

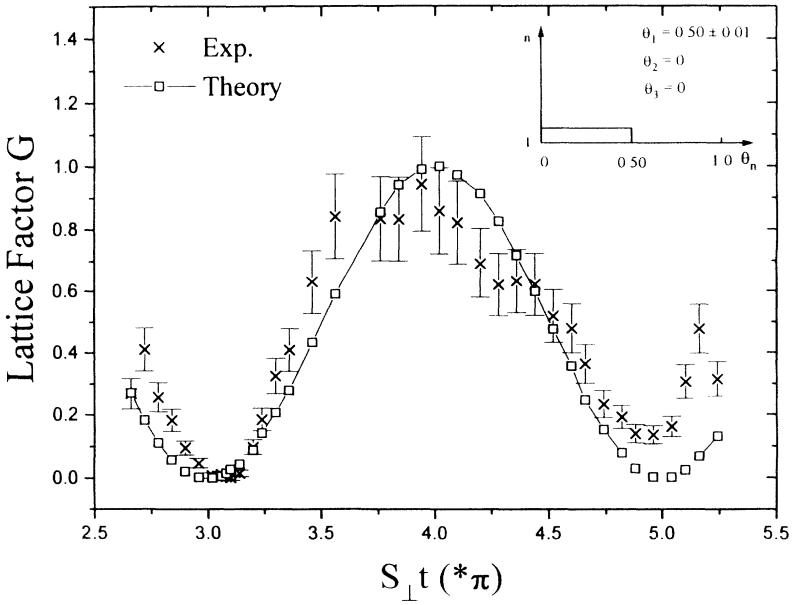

FIG. 3. The lattice G factors obtained from the experimental energy-dependent profiles are shown as crosses. $S_{\perp}t$ is the phase change in the direction perpendicular to the surface. $S_{\perp}$ is the momentum transfer perpendicular to the surface and t is the step height. The solid curve connecting the squares shows the calculated G factor using the vertical-layer distribution shown at the inset where the first layer coverage is about 0.5 ML; the second and third layer coverages are zero.

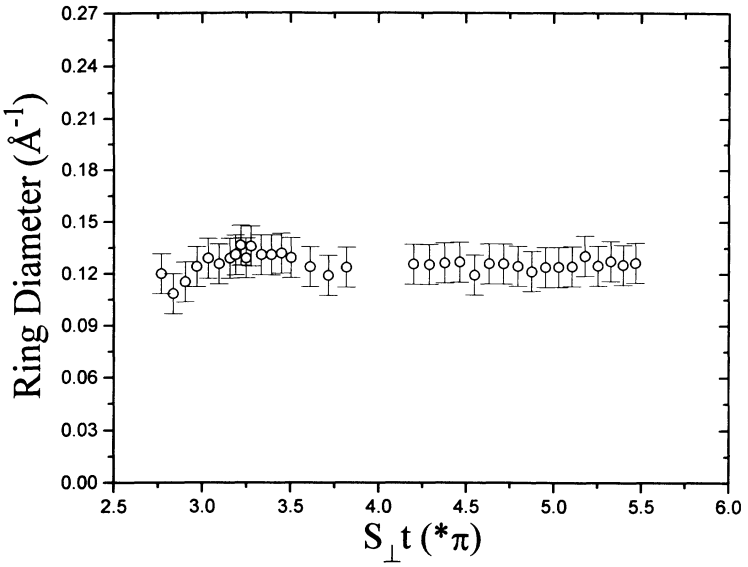

FIG. 4. The spacing between the shoulders (ring diameter) of the (00) beam-diffraction profiles vs energy (phase $S_\perp t$) for about 0.5 ML coverage. There is no data point near the in-phase condition ($\sim 4\pi$) because the profiles are narrow and have no obvious shoulders.

profile is observed, the coverage obtained is 0.496±0.005 ML, which is in surprisingly good agreement with the complete destructive interference of equal number of atoms in two levels, the *G*-factor analysis and the visual inspection of the systematic change in profile's symmetry mentioned earlier.

The optimal Γ distributions of island sizes and spacings at various coverages have been obtained from the profile fits. For example, Fig. 5 shows that the islands grow as a function of coverage (deposition time) and the spacings shrink correspondingly (not shown here). The average island sizes are ~112 and ~146 Å for coverages ~0.21 and ~0.35 ML, respectively. At about 0.50 ML coverage, the average island size and spacing are about the same (~172 Å or ~60 lattice constants for island and ~175 Å or ~61 lattice constants for spacing). We have rescaled the size R by the average island size and replotted the scaled island-size distributions in the upper-right-hand corner of Fig. 5. As one can see, the rescaled island-size distributions superpose on top of each other well, implying that dynamic scaling holds. Similar scaling results were obtained for different deposition rates.

The uniqueness of Γ distribution for islands has been checked in two ways. One is to examine real-space STM images at about 0.50 ML coverage.[11] Although the STM island-size distribution has poorer statistics, it agrees qualitatively with that obtained from the diffraction profile analysis. Another way mentioned earlier is to analyze the energy-dependent profiles (Fig. 2) using the Γ distribution with the same parameters obtained at the out-of-phase condition. All fits show consistently good results. This Γ distribution also resembles the simulation results.[1,2]

There are two possible processes involved in addition to the growth of existing islands: the nucleation of new islands, and the coalescence of two of more islands into one larger island. When the separation of various islands decreases, the islands will likely coalesce to form larger

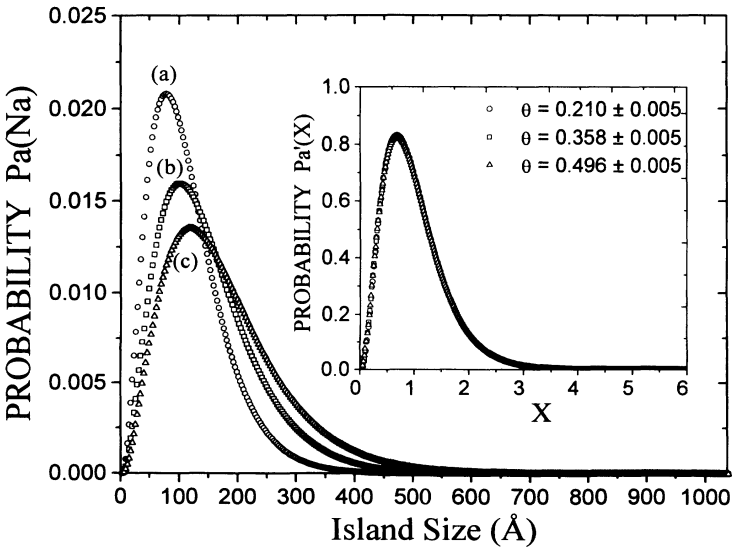

FIG. 5. The coverage-dependent island-size distributions $P_a(R)$ obtained from the fit of measured (00) beam angular profiles. Curves *a*, *b*, and *c* are for coverages 0.210, 0.358, and 0.495, respectively. The inset shows the rescaled island-size distributions $P'_a(x)$.

ones. As the coalescence occurs, the island-size distribution will broaden. It is expected that the system should not exhibit a scaling behavior. We assume the average island size $R' \sim \theta^n$ and the island-size-distribution broadening $\sigma \sim \theta^{n'}$. Plotting the R' and σ obtained from the fit of Γ distribution for coverage range we studied ($0.2 < \theta < 0.5$ ML) in log-log scale, one obtains n and n' from the slopes to be 0.518 and 0.515, respectively. This means there is only one length scale in the scaling and no major islands coalescence occurs for coverage less than 0.5 ML. Reproducible results are also obtained for different deposition rates.

C. Island density $N(\theta)$

Additional information such as the island density $N(\theta)$ can be learned from the scaling of island-size distribution. A simple dimensional analysis tells us the coverage θ equals the total number of islands m times the area of an island R'^2 and then divided by the total area A of the sample, i.e., $\theta = (mR'^2)/A = (m/A)R'^2 = N(\theta)R'^2$. If one assumes that $N(\theta) \sim \theta^q$, then $\theta = \theta^q(\theta^n)^2 = \theta^{q+2n}$. This scaling assumption thus leads to the relation $1 = q + 2n$. If $n = \frac{1}{2}$, then $q = 0$. This means the island density $N(\theta)$ is a constant independent of θ. It was proposed in recent model simulations[1] that in aggregation growth regime if the island density $N(\theta)$ is constant, then one expects the island-size distribution $P_a(\theta)$ to scale with the average island size in a general form, $P_a(\theta) = \theta(R')^{-2} f(R/R')$, where f is the scaling function. If we use the exponent $n = 0.518$ obtained from the coverage-dependent average island size R', we obtained $q = -0.036$. This small negative value means the island density $N(\theta)$ decreases slightly with coverage and is almost a constant. In our case, we estimate the value to be of order 10^{11} cm^{-2} using the average island size and average island spacing obtained from the Γ distributions [e.g., $1/(172+175\ \text{Å})^2$ at ~ 0.5 ML]. This means that in the submonolayer range we studied, the islands are in the aggregation growth regime. If one assumes the separation of shoulder in the profiles of Fig. 1 represents the inverse of average island-island separation, one obtains an almost constant separation consistent with the result of constant island density.

IV. SUMMARY

In summary, we have measured the angular profiles of integral-order diffraction beams from a 1×1 heteroepitaxial layer during submonolayer growth. The fit of calculated intensity profiles to measured profiles provides coverage, island size, and spacing distributions. The island-size distribution and spacing distribution can be best fit by Γ functions. The island-size distribution scales as a function of coverage. The island density is nearly a constant in the aggregation growth regime. If the deposition is performed as function of deposition rate and temperature, many thermodynamic quantities such as activation energy and prefactor can be determined from the scaling behavior. The method is very general and is readily applicable for other submonolayer growth of epitaxial 1×1 layers studied by diffraction techniques.

ACKNOWLEDGMENTS

We acknowledge useful discussions with T.-M. Lu. We also thank J.S. Levinger for reading the manuscript. This work was supported by ONR Grant No. N00014-91-J-1099, and A. Chan was supported by the Department of Education.

[1] J. G. Amar, F. Family, and P.-M. Lam (unpublished); in *Mechanisms of Thin Film Evolution,* edited by S. M. Yalisove, C. V. Thompson, and D. J. Eaglesham, MRS Symposia Proceedings No. 317 (Materials Research Society, Pittsburgh, 1994).

[2] J. W. Evans and M. C. Bartelt, J. Vac. Sci. Technol. A **12**, 1800 (1994); in *Common Themes and Mechanisms of Epitaxial Growth,* edited by P. Fusso, J. Tsaop, D. W. Kisker, A. Zangwill, and T. F. Kvech, MRS Symposia Proceedings No. 312 (Materials Research Society, Pittsburgh, 1993), p. 255; Surf. Sci. **298**, 421 (1993); **284**, L437 (1993); Phys. Rev. B **46**, 12 675 (1992).

[3] J.-K. Zuo, T.-M. Lu, and G.-C. Wang, Phys. Rev. B **39**, 9432 (1989).

[4] H.-J. Ernst, F. Fabre, R. Folkerts, and J. Lapujoulade, J. Vac. Sci. Technol. A **12**, 1809 (1994); Phys. Rev. Lett. **69**, 458 (1992).

[5] H. Busch and M. Henzler, Phys. Rev. B **41**, 4891 (1990).

[6] M. C. Tringides, in Chemical Physics of Solid Surfaces and Heterogeneous Catalysis: Phase Transitions and Adsorbates Restructuring of Metal Surfaces, edited by D. A. King and D. P. Woodruff (Elsevier, Amsterdam, in press), Vol. 6, and references therein.

[7] Y. W. Mo, J. Kleiner, M. B. Webb, and M. G. Lagally, Phys. Rev. Lett. **66**, 1998 (1991); Surf. Sci. **268**, 275 (1992); A. Pimpinelli, J. Villain, and D. E. Wolf, Phys. Rev. Lett. **69**, 985 (1992).

[8] J. A. Stroscio, D. T. Pierce, and R. A. Dragoset, Phys. Rev. Lett. **70**, 3651 (1993); J. A. Stroscio and D. T. Pierce, Phys. Rev. B **49**, 8522 (1994).

[9] J.-K. Zuo and J. F. Wendelken, Phys. Rev. Lett. **66**, 2227 (1991).

[10] W. Li, G. Vidali, and O. Biham, Phys. Rev. B **48**, 8336 (1993).

[11] Q. Jiang, Y.-L. He, A. Chan, and G.-C. Wang, in *Interface Control of Electrical, Chemical, and Mechanical Properties,* edited by S. P. Murarka, T. Ohmi, K. Rose, and T. Seidel, MRS Symposia Proceedings No. 318 (Materials Research Society, Pittsburgh, 1994).

[12] R. L. Schowebel, J. Appl. Phys. **40**, 614 (1969).

[13] J. M. Pimbley and T.-M. Lu, J. Appl. Phys. **57**, 1121 (1985); **58**, 2184 (1985).

[14] J. Wollschlager, J. Falta, and M. Henzler, Appl. Phys. A **50**, 57 (1990); J. Wollschlager and M. Henzler, Phys. Rev. B **39**, 6052 (1989); J. Falta, M. Horn, and M. Henzler, Appl. Surf. Sci. **41/42**, 230 (1989).